Korean J. Chem. Eng., 39(3), 638-645 (2022)
DOI: 10.1007/s11814-021-0966-2

pISSN: 0256-1115
eISSN: 1975-7220

Preparation of chromium fumarate metal-organic frameworks for removal of pharmaceutical compounds from water

Ebru Kurtulbaş*, Selin Şahin*, Mehmet Bilgin*, and Şahika Sena Bayazit,†**

*Istanbul University-Cerrahpaşa, Engineering Faculty, Department of Chemical Engineering, 34320, Avcılar, Istanbul, Turkey
**Beykent University, Faculty of Engineering & Architecture, Department of Chemical Engineering, Istanbul, 34396, Sarıyer, Turkey

(*Received 31 May 2021 • Revised 19 September 2021 • Accepted 27 September 2021*)

Abstract−Pharmaceutical pollution in water is the major cause of antibiotic resistance, so remediation of water from pharmaceuticals is a very important issue. Different methods are used for this purpose, with adsorption as one of the most preferred. Different adsorbents have been used for water treatment processes. Metal-organic frameworks that have highly porous structures have gained attention in the last decades. In this study, novel chromium fumarate (Cr-Fum) was prepared, and the efficiency of Cr-Fum was tested by ciprofloxacin (CPX) adsorption. Cr-Fum was prepared under reflux and characterized by scanning electron microscopy (SEM), X-ray diffraction spectroscopy (XRD), Fourier transform infrared spectroscopy (FTIR), thermal analysis (TGA), and differential scanning calorimetry (DSC). The general approach of the process was monolayer adsorption at low temperature and heterogeneous adsorption at high temperature. 2.5 mg of adsorbent was adsorbed 4.97 mg/g and 11.47% of CPX. 10 mg of Cr-Fum was adsorbed 0.82 mg/g and 7.27% of CPX. Partition coefficients were calculated and 0.07 mg/g/μM was found at 298 K. The reaction followed pseudo-first- and pseudo-second-order kinetic models. Thermodynamic analysis showed that the reaction is spontaneous and exothermic. Additional ions caused decreasing CPX adsorption, but this study showed that Cr-Fum has NaCl adsorption capacity. In future studies, NaCl adsorption should be investigated. Desorption studies were applied to Cr-Fum after the adsorption processes. 0.1 M NaOH and phosphate buffer (pH=7.4) solution were used as desorption eluents. The desorption period was chosen as 6 h. NaOH solution desorbed 67.38% of CPX at first cycle and buffer solution desorbed 26.87% of CPX at second cycle.

Keywords: Metal-organic Frameworks, Ciprofloxacin, Chromium Fumarate, Adsorption

INTRODUCTION

Besides being life-saving chemicals, pharmaceuticals can cause very dangerous pollution, especially in water and soil. Antibiotics also deserve more significant attention because of causing antibiotic-resistant bacteria. There are several ways for revealing pharmaceutical wastes to water and soil. Generally, households and hospitals are the main sources for antibiotics discharging [1]. Also, veterinary usage can be added as another pollution resource. Excessive consumption of antibiotics and lack of wastewater treatment policies can lead to worse health disasters such as epidemics. It is known that pharmaceuticals cannot be metabolized in human and animal bodies, completely [2].

Ciprofloxacin (CPX) is one of the most known and used antibiotics worldwide. A new study reported that CPX is the fifth most commonly consumed antibiotic in the US [3]. CPX can be found in wastewaters of hospitals and pharmaceutical production facilities at high concentrations. According to Li et al., CPX concentrations in wastewaters are nearly 150 μg/L and 50 mg/L in hospitals and pharmaceutical production facilities, respectively [4]. 40-50% of CPX is discharged by the human urine system without any change [5]. Unnecessary contact with CPX can lead to drug resistance in humans. So, purifying wastewaters from pharmaceuticals is very important. Several separation processes are used to develop for the purification of wastewater. Oxidation, adsorption, and coagulation can be given as examples. New porous materials have been developed for adsorption processes in the last decades. Metal-organic frameworks (MOFs) are very important porous material groups for adsorption. In this study, newly prepared chromium fumarate metal-organic frameworks were applied for CPX adsorption.

Metal-organic frameworks are crystalline solids, consisting of metal nodes and organic linkers. Metal nodes and organic ligands link through coordination bonds forming a continuous one-, two-, or three-dimensional porous network [6]. Fumaric acid is one of the organic linkers using the preparation of MOFs. Fe (III) [7], Zr (IV) [8], and In (III) [9] fumarates have been prepared for different aims. Jeyaseelan et al. prepared fumaric-acid based MOFs using Zr^{4+}, La^{3+}, and Fe^{3+} metal nodes and utilized these MOFs for fluoride adsorption [10]. Cr^{3+} metal nodes have not been used for fumaric acid-base MOF preparation until this study. Fumaric acid is also used in foods and drugs. So, fumaric acid can be accepted as a non-toxic organic linker. Various kinds of MOFs have been used for pharmaceutical adsorption. Some Fe-based MOFs were used for CPX adsorption [11]. Also, different kinds of adsorbents have been used for CPX adsorption. Biochar from water hyacinth [12], groundnut shell biosorbent, and ZnO nanoparticles [13] can

†To whom correspondence should be addressed.
E-mail: senabayazit@beykent.edu.tr

be given as examples.

In this study, novel Cr-fum metal-organic frameworks were prepared under reflux. The obtained MOF particles were characterized by SEM, XRD, BET surface area, FTIR, TGA, and DSC methods. Then the adsorption variables of CPX were examined, such as adsorbent quantity, kinetics, isotherm and temperatures.

MATERIALS AND METHODS

1. Materials

The required chemicals for preparation of Cr-fum; Cr (III) nitrate ($Cr(NO_3)_3 \cdot 9H_2O$), methanol (99.9%), ethanol (96%), acetone (>99.5%) and *N,N*-dimethylformamide (99.8%), NaOH (>97%), HCl (37%), Na_2HPO_4 (>99%) and NaH_2PO_4 (>99%) were purchased from Merck Co. Fumaric acid ($C_4H_4O_4$) was obtained from Sigma-Aldrich Co. Ciprofloxacin ($C_{17}H_{18}FN_3O_3 \cdot HCl$) was obtained from Sigma-Aldrich Co. The distilled water was prepared by the Millipore Direct Q-3 system.

2. Methods

Cr-fum was prepared under reflux according to the literature with few differences. Equimolar quantities of $Cr(NO_3)_3 \cdot 9H_2O$ and $C_4H_4O_4$ were dissolved in *N,N*-dimethylformamide (DMF). DMF is a widely used organic solvent for MOF preparation [14]. DMF has unique properties as a polar aprotic solvent. It is hydrophilic and can dissolve most of the organic compounds. It is considered to be an inexpensive solvent in terms of its dissolving power [15]. The mixture was heated at 130 °C for 17 hours under reflux [16]. The obtained solid material was removed from the reaction mixture after cooling to room temperature, washed with acetone and methanol [17], then dried under vacuum (Vacuum oven, Binder) at 60 °C. The product was used by grinding in a mortar.

The chosen characterization methods are scanning electron microscopy (FE-SEM, FEI Quanta FEG 450 at 30 kV), X-Ray diffraction spectroscopy (XRD) (Rigaku D/Max-2200 diffractometer (Cu K_α radiation with λ=0.15418 nm)), BET surface area analysis (Quantachrome Nova 3200e) was applied by N_2 adsorption at 77 K on Cr-Fum. The sample was dried at 60 °C under vacuum before analysis. Fourier transform infrared spectroscopy, FTIR (Bruker Alpha, KBr method), thermogravimetric analysis (Hitachi STA-7200 simultaneous thermogravimetric analyzer; the ramping rate was 10 °C/min in the temperature range of 40-800 °C). Differential scanning calorimetry (DSC 6000, Perkin Elmer) analysis was applied under N_2 atmosphere (20 mL/min, the ramping rate was 10 °C/min in the temperature range of 0-300 °C.

CPX adsorption occurred in batch type. The CPX adsorption efficiencies of Cr-Fum were investigated. For this purpose, some adsorption variables were investigated. Amount of adsorbent, contact time, temperature and CPX concentrations are these variables. Also, the ion effect (NaCl ions) on adsorption was determined. Simultaneously, NaCl adsorption on Cr-fum was investigated. The desorption of CPX molecules on Cr-Fum was studied using two different eluents. These eluents were chosen as 0.1 M NaOH and phosphate buffer solution.

The chosen adsorbent quantities differed between 2.5 mg-10 mg. The initial CPX concentration was 11 mg/L. The reaction temperature was stable at 298 K. The reaction pH was adjusted to 3, and also the reaction lasted for 2 hours according to pre-experiments. Kinetic experiments were carried out at pH=3 and 298 K. The equilibrium time was determined by taking samples at regular intervals and analyzing them. Pseudo-first-order and pseudo-second-order kinetic models were calculated from these experimental results. Isotherm parameters were calculated from experimental results of initial CPX concentration (2-15 mg/L) effects. The chosen models are Langmuir and Freundlich isotherms. NaCl ions (1-10%) were added to CPX adsorption media. After the reaction ended, simultaneously NaCl and CPX adsorption were tested. The ions' effect on CPX adsorption was specified and also NaCl adsorption efficiency of Cr-Fum was investigated. CPX concentration was measured using a UV-Vis spectrophotometer (PG T-60, PG Instruments) directly, at 275 nm [18]. The UV-Vis spectrum of CPX is given in Fig. S1. NaCl concentration was determined by ion-selective electrodes (Hanna Instruments).

The desorption studies were carried on the batch type. After CPX adsorption, Cr-Fum particles were removed, washed with water, and then they were dried under room conditions. The desorption process was started by adding eluent to the dried particles and shaking for 6 hours. The eluent was removed from reaction media and analyzed by UV-Vis spectrophotometer. The same sample was used for CPX adsorption again. This cycle was maintained for three times.

The stability of Cr-Fum was tested by comparing UV-Vis spectra of supernatant of water treated Cr-Fum particles and aqueous Cr(III) solutions. The spectra were obtained by Jasco V-730 UV-Visible spectrophotometer.

The point of zero charge (pH_{pzc}) of Cr-Fum particles was obtained by solid addition method. According to this method, 0.01 M NaCl solution was prepared and the pH values of the solution were adjusted to 2, 4, 6, 8, 10, and 12. 25 mg of Cr-Fum particles were added 20 mL of pH-adjusted NaCl solutions. The mixtures were shaken for 24 hours; then the final pH values were analyzed by pH-meter (WTW GMBH, Germany). The plot was drawn between initial pH and ΔpH. The intersection point of ΔpH=0 and curve gave the pH_{pzc} [19].

RESULTS

1. Characterization of Cr-Fum Particles

SEM image of Cr-Fum particles can be seen in Fig. 1. According to the literature of fumarate-based MOFs [20], the shape of fumarates is generally between smooth structure and crystalline structure. As explained by Karmakar et al., the morphology of Cr-Fum is neither crystalline nor smooth [20]. The structure of obtained powder Cr-Fum is compatible with the literature.

Cr-Fum MOFs were developed according to literature and only one method was chosen for production. In this study, DMF was chosen as solvent and reaction time was chosen as 17 hours. The solvent media and the reaction time are affected the crystal shape of Cr-Fum. In Fig. 2, XRD patterns of Cr-Fum were given. Cr-Fum MOF peaks can be seen at 10.79°, 21.72° [21]. But the noise of the pattern is explained by the reaction conditions. Horcajada et al. proved that reaction time increased the crystallinity of fumarate MOFs [22].

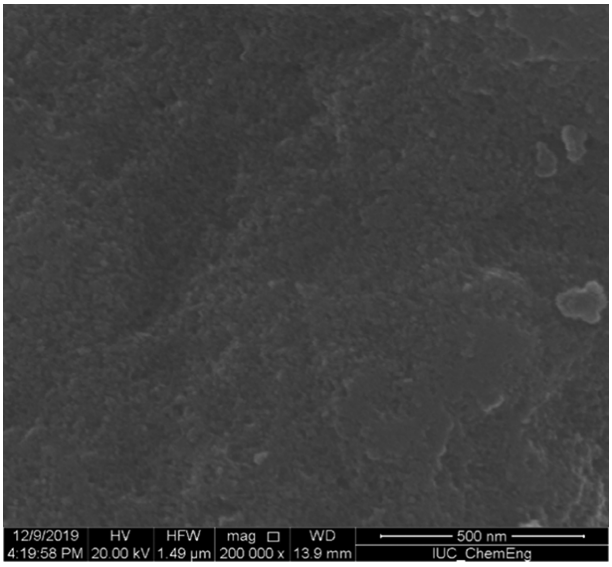

Fig. 1. SEM images of Cr-Fum particles (200,000 magnitude).

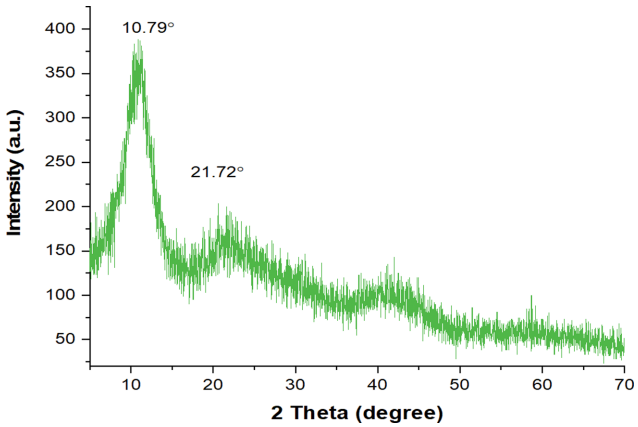

Fig. 2. XRD pattern of Cr-Fum particles.

BET surface area of Cr-Fum was determined as 30.35 m^2/g. According to the other fumarates mentioned in the literature, the surface area of Cr-Fum is very low. But also, there are some MOFs that have low surface area that can be encountered in literature [23]. The synthesis method and the purification step should be developed in further studies.

FTIR plots of Cr-Fum and fumaric acid are given in Fig. 3(a). The peak at 548 cm^{-1} is indicative of Cr-C stretch and the peak at 3,463 cm^{-1} pointed out -OH stretching. Generally, Cr-C stretching absorptions can be observed between 300-800 cm^{-1} [24]. And also, Cr-H stretching absorptions can be observed between 800-600 cm^{-1} [25]. The peak at 688 cm^{-1} is C=C bending; 1,401 and 1,522 cm^{-1} are connected by symmetric and asymmetric COO- stretching, respectively. It can be understood that Cr-Fum MOFs occurred. The adsorption mechanism was estimated according to FTIR plots of before and after CPX adsorption on Cr-Fum. These plots are given in Fig. 3(b). After the adsorption process, -OH stretching peak at 3,437 cm^{-1} occurred. The intensity of 1,401, 1,417 and 1,522 cm^{-1} peaks decreased after CPX adsorption. The adsorption process can progress on the chemical attraction between CPX molecule and carboxylic groups of Cr-Fum.

Thermal analysis of Cr-Fum particles is illustrated in Fig. 4. As seen in TG plots, the moisture quantity of Cr-Fum was about 7% and thermal degradation started at 422 °C according to DTG plots. 40% of Cr-Fum is dependent on the metallic part of MOF and approximately 60% of Cr-Fum is the organic part of MOF. Non-isothermal DSC curve is given in Fig. S2. The glass transition temperature was 101.88 °C. DSC curve shows the exothermic peak at this temperature. It was noticed that there was not seen weight loss or endothermic peak below the temperature. That means there were no coordinated or free water molecules in Cr-Fum [26].

The stability of Cr-Fum towards the water was investigated. UV-Vis spectrum of aqueous Cr(III) ions is given in Fig. S3. The characteristic peaks of Cr(III) at 420 and 580 nm are seen in figure. These peaks were supported by the literature [27]. Cr-Fum particles were shaken in water during optimum adsorption reaction and then the supernatant was obtained and scanned by UV-

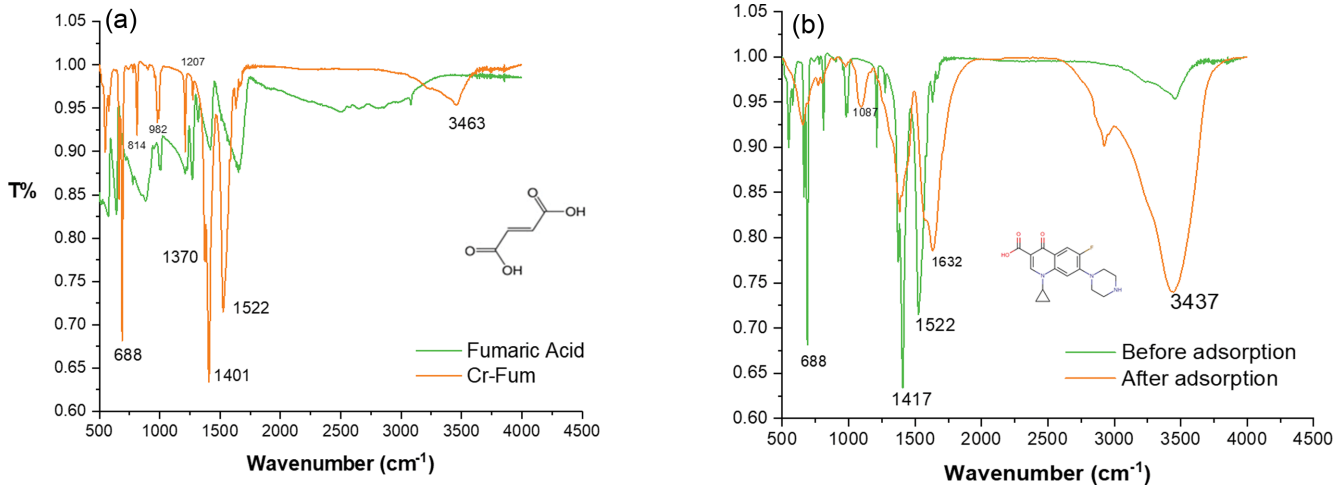

Fig. 3. FTIR plots of fumaric acid and Cr-Fum (a), molecular structure of fumaric acid was obtained from [38]; FTIR plots of before and after CPX adsorption of Cr-Fum particles. (b) can be added here.

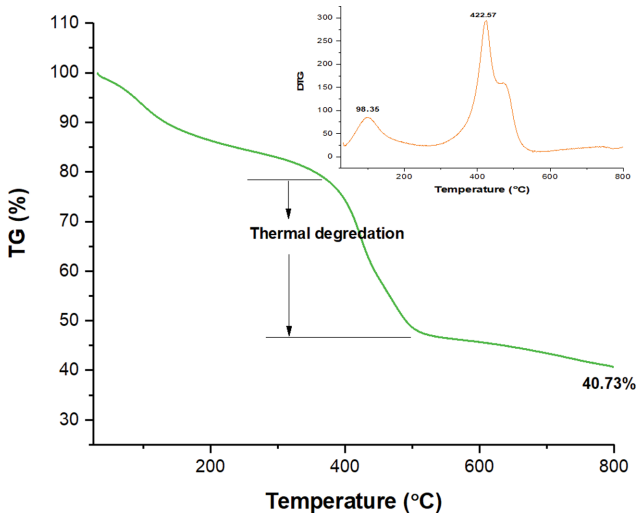

Fig. 4. TGA and DTG plots of Cr-Fum.

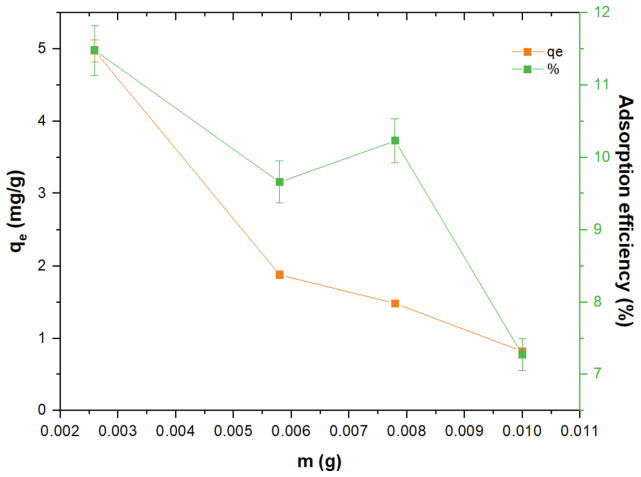

Fig. 5. Adsorbent quantity effect on CPX adsorption.

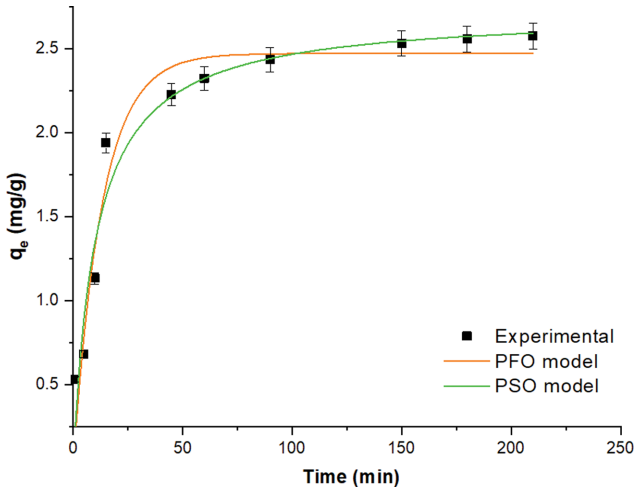

Fig. 6. Contact time experimental results and PFO and PSO kinetic model plots.

Vis. The spectrum is given in Fig. S2. And it was understood that Cr(III) ions were stable in Cr-Fum particles because no similar or other peaks were seen.

2. Analysis of CPX Adsorption and Desorption Variables on Cr-Fum Particles

The adsorbent quantity effect is one of the adsorption variables investigated in this study. The chosen quantities are 2.5-10 mg. Analysis of adsorption is calculated by using the following equations.

$$q_e \times m = (C_0 - C_e) \times V \quad (1)$$

$$\text{CPX Removal (\%)} = \frac{C_0 - C_e}{C_0} \times 100 \quad (2)$$

C_0 and C_e (mg/L) are initial and equilibrium concentrations of CPX, q_e (mg/g) is adsorption uptake, m (g) is the adsorbent quantity and V (L) is solution volume. 2.5 mg of adsorbent was adsorbed 4.97 mg/g and 11.47% of CPX. 10 mg of Cr-Fum was adsorbed 0.82 mg/g and 7.27% of CPX (Fig. 5).

The experiments of equilibrium time determination provide the calculation of kinetic models. PFO and PSO models were applied to experimental data.

$$q_t = q_e \times (1 - e^{-k_1 \times t}) \quad (3)$$

Eq. (3) shows Lagergren pseudo-first-order kinetic model [28]. q_t and q_e (mg/g) are adsorption uptake at t time and at equilibrium. k_1 (min^{-1}) is PFO rate constant

$$q_t = \frac{q_e^2 \times k_2 \times t}{1 + k_2 q_e t} \quad (4)$$

Eq. (4) is a pseudo-second-order kinetic model [29]. k_2 (g/mg) is PSO rate constant. The kinetic plots are given in Fig. 6 and the calculated parameters are presented in Table 1. The equilibrium time was determined as 120 min. According to R^2 values (0.94), the adsorption process follows PFO and PSO models. Calculated q_e values are 2.47 mg/g at PFO and 2.72 mg/g at PSO. These values are compatible with experimental results. Chemisorption is the rate-limiting step.

Isotherm models plots are given in Fig. 7 and calculated parameters are shown in Table 2. Langmuir [30] (Eq. (5)) and Freundlich

Table 1. Kinetic parameters of CPX adsorption

	Pseudo first-order kinetic model		Pseudo second-order kinetic model	
Cr-Fum	q_e (mg/g)	2.47	q_e (mg/g)	2.72
	k_1 (min^{-1})	0.076	k_2 (g/mg min)	0.036
	Adj. R^2	0.94	Adj. R^2	0.94
	Red. Chi-Sqr	0.037	Red. Chi-Sqr	0.0035

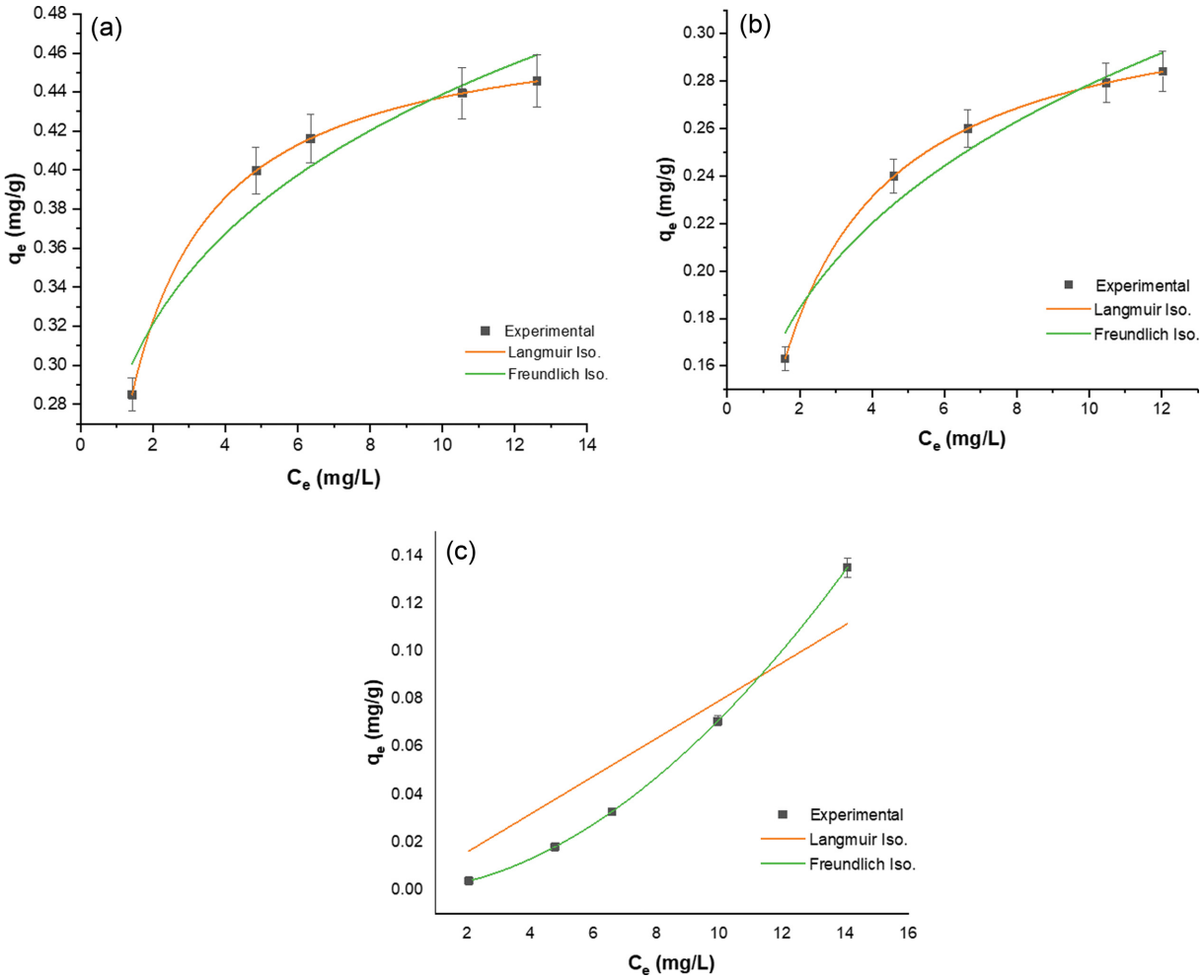

Fig. 7. Isotherm plots of CPX adsorption on Cr-Fum, at 298 K (a), 303 K (b), 313 K (c).

Table 2. Isotherm parameters of CPX adsorption at 298, 303 and 313 K

		Temperature (K)		
		298	303	313
Langmuir isotherm	q_m	0.48	0.32	-
	K_L	1.03	0.65	4.5×10^{-6}
	Adj. R^2	0.99	0.99	0.81
	Red. Chi-Sqr	7.2×10^{-32}	1.87×10^{-31}	5.18×10^{-4}
Freundlich isotherm	K_f	0.28	0.15	9.67×10^{-4}
	n	5.16	3.89	0.54
	Adj. R^2	0.92	0.94	0.99
	Red. Chi-Sqr	3.28×10^{-4}	1.38×10^{-4}	3.44×10^{-33}

[31] (Eq. (6)) isotherms at three different temperatures were applied.

$$q_e = \frac{q_m \times K_L \times C_e}{1 + K_L \times C_e} \quad (5)$$

$$q_e = K_F \times C_e^{1/n} \quad (6)$$

$$PC = \frac{q_e}{C_e} \quad (7)$$

In Eq. (5), q_m is the theoretical maximum adsorption capacity (mg/g), K_L is the equilibrium adsorption constant (L/mg). In Eq. (6), K_F is Freundlich constant ((mg/g)(L/g)^n), n is the heterogeneity factor. CPX adsorption reaction on Cr-Fum followed monolayer process according to Langmuir isotherm because of high R^2 values at 298 and 303 K. When the temperature increased (313 K), adsorption uptake values decreased and Freundlich isotherm was suitable for the process. Increasing the temperature causes decreas-

Table 3. The literature comparison table of CPX adsorption capacities of different adsorbents

Adsorbent	q_m (mg/g)	pH	Temperature (°C)	Ref.
Carbon nanofibers	10.36	5.0	25	[4]
Schorl	8.49	5.5	-	[11]
Clinoptilolite	5.31	6.0	25	[11]
MgO nanoparticles	3.46	2.0	-	[11]
Biochar from water hyacinth	2.71	4.0	25	[12]
Groundnut shell biosorbent	0.6	6.0	25	[11]
ZnO nanoparticles	0.16	6.0	25	[11]
Cr-Fum	0.48	3.0	25	This work

ing in adsorption efficiency. The increasing energy of the system is concluded desorption of adsorbed molecules on solid particles [32]. The adsorption efficiency of Cr-Fum particles can be compared by the literature. In Table 3, some examples are given according to their Langmuir q_m values and physical conditions such as pH and temperature. It can be seen that Cr-Fum particles have improved adsorption efficiency over some metal oxides (ZnO) and natural biosorbents.

The partition coefficient (PC) was explained by Na et al., as applying for evaluating adsorption performance at an equivalent level to overcome the limitation based on the adsorption capacity concept [33]. Szulejko et al. reported that PC values are the most effective parameters than BET surface areas [34]. According to Eq. (7), the ratio of adsorption capacity and final concentration gives the PC value (mg/g/μM). The calculated PC values of equilibrium data are given in Table S1 with all experimental data. And the effect of initial CPX concentration on PC is presented in Fig. S4. As seen in the figure, lower initial CPX concentration and lower temperature are very suitable for CPX adsorption. PC values range from 0.01-0.07 at 298 K and 0.001-0.0003 at 313 K. Temperature increasing is not a proper choice for increasing the CPX adsorption efficiency on Cr-Fum.

ΔG, ΔH, and ΔS were calculated by thermodynamic analysis. Eqs. (7) and (8) were used for analysis.

$$\ln K = -\frac{\Delta H}{RT} + \frac{\Delta S}{R} \quad (8)$$

$$\Delta G = -RT\ln K \quad (9)$$

Langmuir parameter K_L was used for Eq. (8) (van't Hoff eq.) and (9). The plot between 1/T and lnK provides the calculation of ΔH and ΔS. The calculated parameters are given in Table 4. ΔG values were generally negative at high temperature; this situation can be explained that the process was spontaneous [35]. And the process was identified as exothermic according to ΔH (−677.39 kJ/mol). The magnitude of ΔH values can give an idea about the mechanism of the adsorption process. The adsorption occurs by chemisorption. Negative ΔS values show decreasing the randomness of the adsorption process [35].

Co-existing ion effect was investigated by adding NaCl into the adsorption media. The salt concentrations were chosen as 1,5 and 10%. CPX and NaCl were adsorbed simultaneously. The results are given in Fig. 8. The increasing NaCl concentration caused the decreasing CPX adsorption. Because NaCl ions are adsorbed on Cr-Fum particles. The NaCl adsorption reached 62% of efficiency while the initial NaCl concentration was 1%.

Table 4. Thermodynamic parameters of CPX adsorption on Cr-Fum particles

ΔG (J/mol)	298 K	73.23
	303 K	−1,085.2
	313 K	−32,037.8
ΔH (kJ/mol)		−677.39
ΔS (kJ/mol K)		−2.26

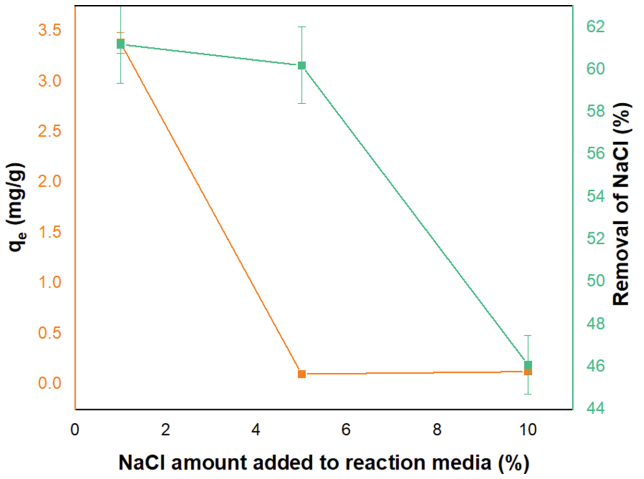

Fig. 8. NaCl effect on CPX adsorption and NaCl adsorption on Cr-Fum.

The most efficient adsorption results were obtained at pH=3. So, all the process was carried out at this pH value. The pH_{pzc} value of Cr-Fum particles was found as 5.1 (Fig. S5). Below the pH_{pzc} value, the surface of Cr-Fum is positively charged. If the surface is positively charged, the CPX adsorption mechanism is due to complex interactions by deprotonated carboxylic groups [11,36]. This result is in line with the FTIR result.

0.1 M NaOH and phosphate buffer solution were used for CPX desorption on Cr-Fum particles. The desorption efficiency of eluents was determined according to following equation (Eq. (10)) [37];

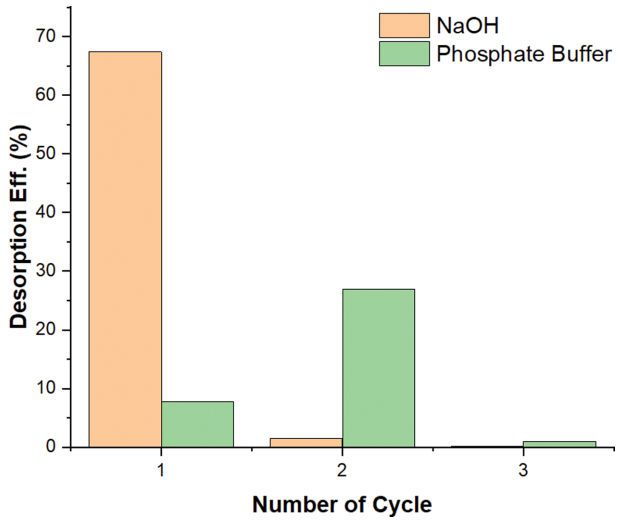

Fig. 9. Desorption of CPX molecules from Cr-fum by 0.1 M NaOH and phosphate buffer (pH=7.4) solution.

$$\text{desorption eff.} = \frac{\text{amount of desorbed COX}}{\text{amount of adsorbed CPX}} \times 100 \quad (10)$$

The plots of desorption efficiency are illustrated in Fig. 9. 0.1 M NaOH solution was very efficient at the first cycle. The desorption ratio was 67.38%, but at the second cycle the efficiency of the solution decreased sharply. The phosphate buffer solution was chosen as the other eluent. This eluent showed lower desorption ability than NaOH solution. At the first cycle, the desorption ratio of phosphate buffer solution was 7.75% and at the second cycle, the desorption ratio was 26.87%. At the third cycle, both of the eluents could not desorb CPX molecules efficiently. Adsorption efficiency also decreased with desorption processes.

CONCLUSION

Chromium fumarate as an adsorbent was prepared by reflux method in DMF solvent. The obtained particles were analyzed by SEM, XRD, FTIR, and TGA. Cr-Fum particles were prepared for the first time in this study and tested for CPX adsorption ability. CPX adsorption on Cr-Fum was investigated by adsorbent quantity, contact time, temperature, initial CPX concentration. 2.5 mg of adsorbent was adsorbed 4.97 mg/g of CPX. 10 mg of Cr-Fum was adsorbed 0.82 mg/g of CPX. The equilibrium time was determined as 120 min. The adsorption process follows PFO and PSO models. The calculated q_e values are compatible with experimental results. CPX adsorption reaction followed monolayer process according to Langmuir isotherm because of R^2 values at 298 and 303 K. Thermodynamic analysis showed that the reaction is spontaneous and exothermic. Additional ions caused decreasing CPX adsorption, but this study showed that Cr-Fum has NaCl adsorption capacity. In future studies, NaCl adsorption should be investigated. 0.1 M NaOH and phosphate buffer solutions were used for desorption process. The desorption rate of NaOH was very high at first cycle, and the desorption rate of phosphate buffer was lower than NaOH solution.

DECLARATIONS

Funding: Not applicable

Conflicts of interest/Competing interests: The authors declare that they have no conflict of interest.

Availability of data and material (data transparency): Not applicable

Code availability (software application or custom code): Not applicable

Authors' contributions: Ebru Kurtulbaş: Methodology, data analysis; Selin Şahin: Conceptualization, methodology, writing-review and editing; Mehmet Bilgin: Writing-review and editing; Şahika Sena Bayazit: Conceptualization, methodology, writing-review and editing

Additional declarations for articles in life science journals that report the results of studies involving humans and/or animals: Not applicable

Ethics approval : Not applicable

Consent to participate: Not applicable

Consent for publication: Not applicable

SUPPORTING INFORMATION

Additional information as noted in the text. This information is available via the Internet at http://www.springer.com/chemistry/journal/11814.

REFERENCES

1. K. Kümmerer, *Chemosphere*, **45**, 957 (2001).
2. K. Kümmerer, *Sustain. Chem. Pharm.*, **12**, 100136 (2019).
3. S. K. Mondal, A. K. Saha and A. Sinha, *J. Clean. Prod.*, **171**, 1203 (2018).
4. X. Li, W. Wang, J. Dou, J. Gao, S. Chen, X. Quan and H. Zhao, *J. Water Process Eng.*, **9**, e14 (2016).
5. G. Jilany Khan, R. Ahmad Khan, I. Majeed, F. Ahmed Siddiqui and S. Khan, *Prof. Med. J.*, **22**, 1 (2015).
6. L. G. Gordeeva, Y. D. Tu, Q. Pan, M. L. Palash, B. B. Saha, Y. I. Aristov and R. Z. Wang, *Nano Energy*, **84**, 105946 (2021).
7. T. Chalati, P. Horcajada, R. Gref, P. Couvreur and C. Serre, *J. Mater. Chem.*, **21**, 2220 (2011).
8. G. Zahn, P. Zerner, J. Lippke, F. L. Kempf, S. Lilienthal, C. A. Schröder, A. M. Schneider and P. Behrens, *CrystEngComm*, **16**, 9198 (2014).
9. Y. Zhang, B. E. G. Lucier, S. M. McKenzie, M. Arhangelskis, A. J. Morris, T. Friščić, J. W. Reid, V. V. Terskikh, M. Chen and Y. Huang, *ACS Appl. Mater. Interfaces*, **10**, 28582 (2018).
10. A. Jeyaseelan, M. Naushad and N. Viswanathan, *J. Chem. Eng. Data*, **65**, 2990 (2020).
11. C. A. Igwegbe, S. N. Oba, C. O. Aniagor, A. G. Adeniyi and J. O. Ighalo, *J. Ind. Eng. Chem.*, **93**, 57 (2021).
12. E. C. Ngeno, F. Orata, L. D. Baraza, V. O. Shikuku and S. J. Kimosop, *J. Chem. Chem. Eng.*, **10**, 185 (2016).
13. N. Dhiman and N. Sharma, *Indian Chem. Eng.*, **61**, 67 (2019).
14. Z. P. Wu, M. X. Wang, L. J. Zhou, Z. L. Yin, J. Tan, J. L. Zhang and Q. Y. Chen, *Trans. Nonferrous Met. Soc. China (English Ed.)*, **24**,

3722 (2014).
15. M. M. Heravi, M. Ghavidel and L. Mohammadkhani, *RSC Adv.*, **8**, 27832 (2018).
16. B. Bozbiyik, J. Lannoeye, D. E. De Vos, G. V. Baron and J. F. M. Denayer, *Phys. Chem. Chem. Phys.*, **18**, 3294 (2016).
17. H. W. B. Teo, A. Chakraborty, Y. Kitagawa and S. Kayal, *Int. J. Heat Mass Transf.*, **114**, 621 (2017).
18. Y. Sun, H. Li, G. Li, B. Gao, Q. Yue and X. Li, *Bioresour. Technol.*, **217**, 239 (2016).
19. A. Xie, J. Dai, X. Chen, J. He, Z. Chang, Y. Yan and C. Li, *RSC Adv.*, **6**, 72985 (2016).
20. S. Karmakar, J. Dechnik, C. Janiak and S. De, *J. Hazard. Mater.*, **303**, 10 (2016).
21. R. Azhdari, S. M. Mousavi, S. A. Hashemi, S. Bahrani and S. Ramakrishna, *J. Environ. Chem. Eng.*, **7**, 103437 (2019).
22. P. Horcajada, T. Chalati, C. Serre, B. Gillet, C. Sebrie, T. Baati, J. F. Eubank, D. Heurtaux, P. Clayette, C. Kreuz, J.-S. Chang, Y. K. Hwang, V. Marsaud, P.-N. Bories, L. Cynober, S. Gil, G. Férey, P. Couvreur and R. Gref, *Nat. Mater.*, **9**, 172 (2010).
23. V. Gargiulo, M. Alfè, F. Raganati, L. Lisi, R. Chirone and P. Ammendola, *Fuel*, **222**, 319 (2018).
24. V. Jonas and W. Thiel, *J. Chem. Phys.*, **102**, 8474 (1995).
25. K. Nakamoto, *Infrared and raman spectra of inorganic and coordination compounds*, in: Ed. by P. R. Griffiths, Handb. Vib. Spectrosc., John Wiley & Sons, Ltd, Chichester, UK (2006).
26. F. Zhang, D. Jiang and X. Zhang, *Nano-Structures and Nano-Objects*, **5**, 1 (2016).
27. A. L. Petrou, V. Thoma and K. Tampouris, *Bioinorg. Chem. Appl.*, **2010**, (2010).
28. S. Lagergren, *K. Sven. Vetenskademiens Handl.*, **24**, 1 (1898).
29. Y.-S. Ho, *J. Hazard. Mater.*, **136**, 681 (2006).
30. I. Langmuir, *J. Am. Chem. Soc.*, **40**, 1361 (1918).
31. H. Freundlich, *Zeitschrift F{ü}r Phys. Chemie*, **57**, 385 (1906).
32. M. H. Jnr and A. I. Spiff, *Electron. J. Biotechnol.*, **8**, 717 (2005).
33. C. J. Na, M. J. Yoo, D. C. W. Tsang, H. W. Kim and K. H. Kim, *J. Hazard. Mater.*, **366**, 452 (2019).
34. J. E. Szulejko, K. H. Kim and J. Parise, *Sep. Purif. Technol.*, **212**, 980 (2019).
35. I. Anastopoulos and G. Z. Kyzas, *J. Mol. Liq.*, **218**, 174 (2016).
36. H. Li, D. Zhang, X. Han and B. Xing, *Chemosphere*, **95**, 150 (2014).
37. V. K. Gupta and A. Rastogi, *J. Hazard. Mater.*, **154**, 347 (2008).
38. I. Goldberg and J. S. Rokem, *Organic and fatty acid production, microbial*, in: Encycl. Microbiol., Elsevier Inc., Amsterdam (2009).

Supporting Information

Preparation of chromium fumarate metal-organic frameworks for removal of pharmaceutical compounds from water

Ebru Kurtulbaş*, Selin Şahin*, Mehmet Bilgin*, and Şahika Sena Bayazit,†**

*Istanbul University-Cerrahpaşa, Engineering Faculty, Department of Chemical Engineering, 34320, Avcılar, Istanbul, Turkey
**Beykent University, Faculty of Engineering & Architecture, Department of Chemical Engineering, Istanbul, 34396, Sarıyer, Turkey
(*Received 31 May 2021 • Revised 19 September 2021 • Accepted 27 September 2021*)

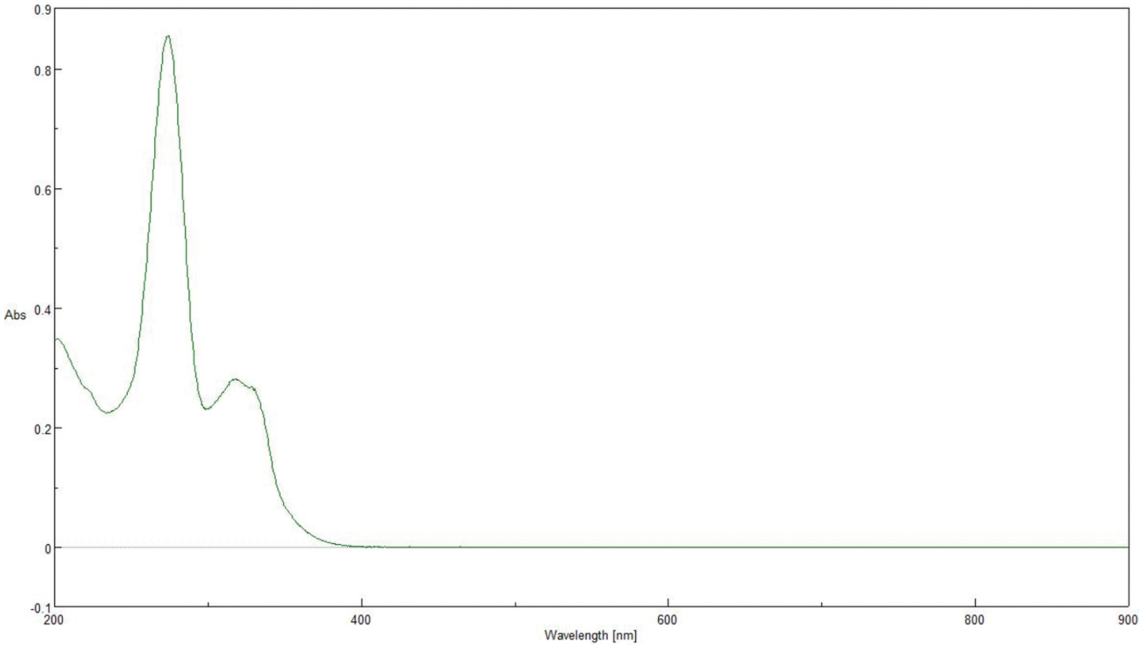

Fig. S1. UV-Vis spectrum of CPX.

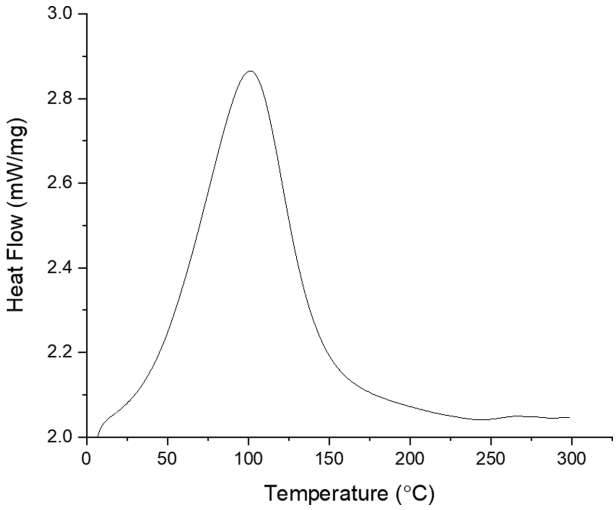

Fig. S2. DSC curve of Cr-Fum nanoparticles.

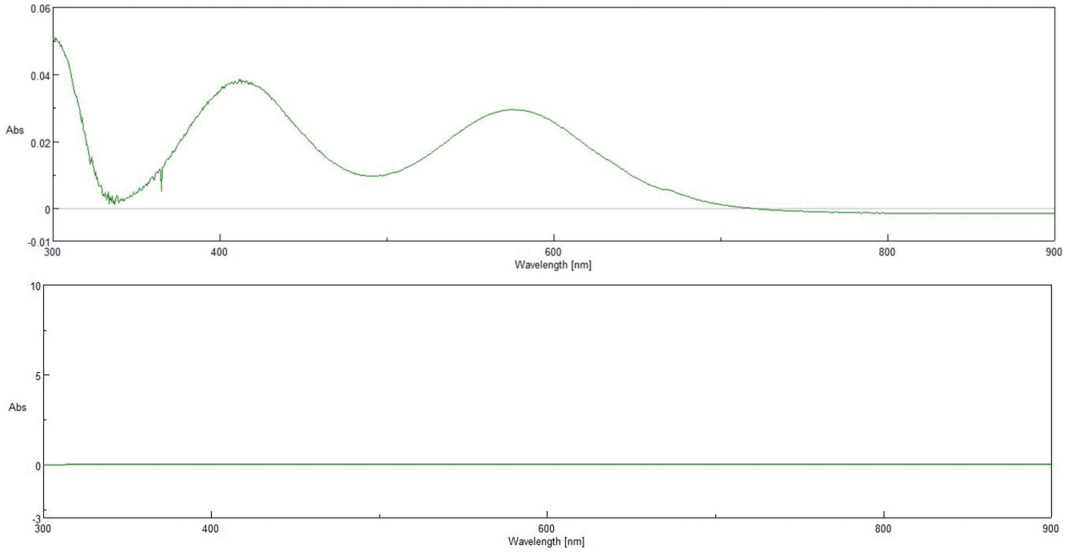

Fig. S3. The spectrum plots of aqueous Cr(III) ions and water treated Cr-Fum.

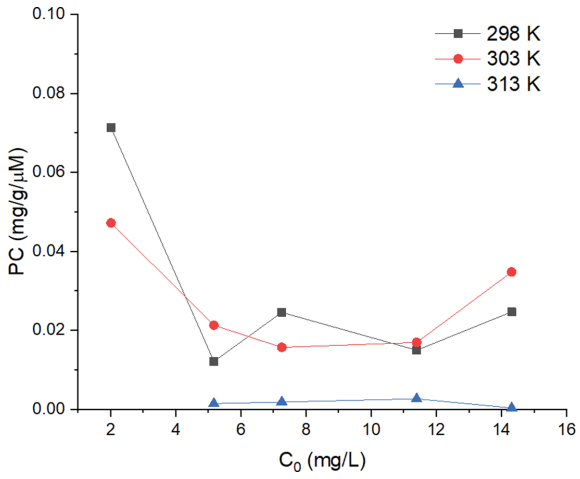

Fig. S4. The PC-C0 plots of CPX adsorption on Cr-Fum.

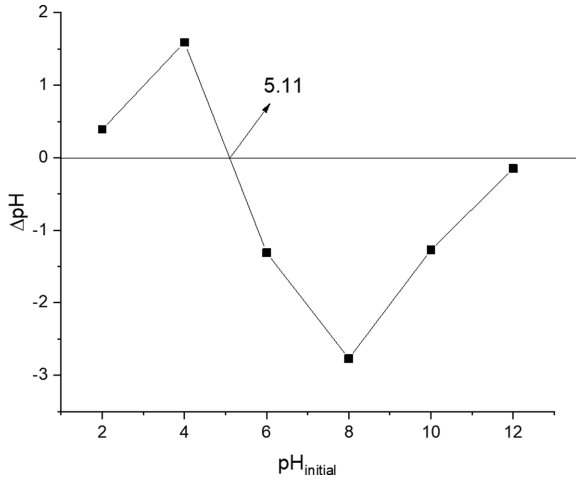

Fig. S5. pH_{pzc} plot of Cr-Fum nanoparticles.

Table S1. Experimental data of equilibrium isotherm studies for CPX adsorption onto Cr-Fum (pH=3)

Temperature (K)	m (g)	C_0 (mg L^{-1})	C_e (mg L^{-1})	q_e (mg g^{-1})	PC (mg g^{-1} μM^{-1})
298	0.0201	14.313	12.613	0.846	0.0246
	0.0200	11.398	10.541	0.428	0.0149
	0.0211	7.254	6.359	0.424	0.0245
	0.0200	5.170	4.850	0.159	0.0121
	0.0213	2.012	1.423	0.276	0.0713
303	0.0200	14.313	12.037	1.138	0.035
	0.0191	11.398	10.477	0.482	0.017
	0.0212	7.254	6.653	0.283	0.016
	0.0211	5.170	4.607	0.266	0.021
	0.0199	2.012	1.602	0.206	0.047
313	0.204	14.313	14.070	0.012	0.0003
	0.204	11.398	9.953	0.071	0.0026
	0.205	7.254	6.590	0.032	0.0018
	0.209	5.170	4.786	0.018	0.0014